Investigational New Drugs (2019) 37:1146–1157
https://doi.org/10.1007/s10637-019-00740-4

PRECLINICAL STUDIES

Synergistic effect and reduced toxicity by intratumoral injection of cytarabine-loaded hyaluronic acid hydrogel conjugates combined with radiotherapy on lung cancer

Juan Tang[1] · Na Wang[1] · JingBo Wu[1] · PeiRong Ren[1] · JunYang Li[1] · LiShi Yang[1] · XiangXiang Shi[1] · Yue Chen[2] · ShaoZhi Fu[1] · Sheng Lin[1,2]

Received: 12 December 2018 / Accepted: 1 February 2019 / Published online: 21 February 2019

Summary

The aim of this study was to explore the synergistic anti-tumor effects of cytarabine hyaluronic acid-tyramine (Ara-HA-Tyr) hydrogel conjugates and radiotherapy (RT) in the Lewis lung cancer (LLC) xenograft model, and the mechanisms involved. The radiotherapy sensitization ratio (SER) of 0.5 μg cytarabine (Ara-C) was 1.619 in the LLC cells. Ara-HA-Tyr was prepared by encapsulating Ara-C into hyaluronic acid-tyramine (HA-Tyr) conjugates. The hydrogels were formed through the oxidative coupling of tyramines by hydrogen peroxide (H_2O_2) and horseradish peroxidase (HRP). Mice engrafted with the LLC cells were given intra-tumoral injections of saline, Ara-C or Ara-HA-Tyr, with or without RT. The combination of Ara-HA-Tyr and RT increased survival compared to free Ara-C and RT ($p < 0.05$), and prolonged tumor growth delay (TGD). Furthermore, the RT + Ara-HA-Tyr combination therapy significantly reduced ^{18}F-FDG uptake, induced cell cycle arrest at G2/M-phase, increased apoptosis and histone H2AX phosphorylation (γ-H2AX), and decreased the proliferation index (Ki67) in tumor cells compared to either monotherapy. Taken together, Ara-C encapsulated with HA-Tyr effectively sensitized tumor xenografts to RT and showed significantly less systemic toxicity.

Keywords Cytarabine · Hydrogel · Radiotherapy · Synergistic effect

Introduction

Radiotherapy (RT) has been the mainstay of non-surgical cancer therapy for over a century [1]. Although the equipment and techniques of RT have improved considerably, the local control rate and overall patient survival rate remain unsatisfactory. Several radio-sensitizing anti-cancer drugs have therefore been developed to optimize RT outcome [2]. Cytarabine, or cytosine arabinoside (Ara-C), is a nucleoside analog and the backbone of acute myeloid leukemia (AML) induction and consolidation therapies [3], and has also shown good therapeutic effect against pleural effusion caused by lung cancer [4]. However, Ara-C has a short half-life and is rapidly inactivated by deoxycytidine deaminase (DCD) outside the target cells, which restricts its use in solid tumors. Furthermore, its lack of selective distribution in vivo results in low intra-tumoral drug concentrations and toxicity to normal tissues. To overcome the short half-life and toxicity of Ara-C, liposomal encapsulated forms were developed, which showed better therapeutic effect compared to the free drug in CNS leukemia/lymphoma [5, 6]. Since solid tumors are resistant to Ara-C therapy in the recommended doses, it is of interest to consider a higher-dose therapy in solid tumors [7]. Furthermore, changes in the route of administration may also affect Ara-C metabolism in vivo. Taken together, the half-life of Ara-C can be extended and its anti-tumor effect can be

Highlights
- Cytarabine has radio-sensitizing abilities on Lewis lung cancer cells.
- Hyaluronic acid–tyramine conjugates as a cytarabine carrier for intratumoral injection.
- The complexes exhibited radiotherapy sensitization and prolonged the survival time.

Juan Tang and Na Wang have contributed equally to this work

✉ ShaoZhi Fu
shaozhifu513@163.com

✉ Sheng Lin
lslinsheng@163.com

[1] Department of Oncology, Affiliated Hospital of Southwest Medical University, 25 TaiPing Rd, Luzhou 646000, China

[2] Nuclear Medicine and Molecular Imaging Key Laboratory of Sichuan Province, Affiliated Hospital of Southwest Medical University, Luzhou 646000, China

increased (without increasing toxicity of higher doses), by incorporating a cancer cell-targeting feature and modifying its delivery mode.

Hyaluronic acid (HA) is a linear muco-polysaccharide consisting of multiple disaccharide units of glucuronic acid and N-acetylglucosamine. It has good biocompatibility, biodegradability, high visco-elasticity and binds to specific cell surface receptors. Currently, hyaluronates are used for treating osteoarthritis, embryo implantation, wound healing etc. [8, 9]. In addition, studies show high efficacy of sodium hyaluronate and hyaluronan nanoparticles in delivering functional genes and chemotherapeutics [10, 11]. The advantage of hydrogel technology is the in situ cross-linking between the gel precursor and a bioactive agent, which obviates the shortcomings of semi-solid hydrogels that cannot be injected [12, 13]. However, injectable hydrogel systems also have the disadvantage of uncontrolled, rapid drug release. Since they typically contain a higher concentration of drugs than that in bolus injections, rapid drug release could lead to off-site accumulation and potential overdose. This drawback not only limits the therapeutic efficacy of the hydrogel systems but also make them unsuitable for delivering drugs with a narrow therapeutic index. Kurisawa et al. developed an injectable, biodegradable and chemically crosslinked hydrogel delivery system made of hyaluronic acid–tyramine conjugates (HA–Tyr) [14, 15], which released the drug cargo in a sustained manner. In this study, we encapsulated Ara-C in the HA–Tyr hydrogel for a sustained and targeted release, and analyzed its radiosensitization capacity and toxicity in both in vitro and in vivo models of lung cancer.

Materials and methods

Reagents and cell lines

Cytarabine (>99%), HA (>95%, Mw = 90KDa), Tyramine hydrochloride (Tyr·HCl), N-hydroxysuccinimide (NHS), 1-ethyl-3-(3-dimethylaminopropyl)-carbodiimide hydrochloride (EDC·HCl), hydrogen peroxide (H_2O_2), horseradish peroxidase (HRP, 100 U/mg) and bovine testicular hyaluronidase were all purchased from MeiLun Co. Ltd. (Dalian, China). Phosphate buffered saline (PBS) was purchased from Sigma-Aldrich Inc. (St. Louis, MO). Dimethyl sulfoxide (DMSO) and crystal violet were purchased from Kelong Co. Ltd. (Chengdu, China). Polyclonal antibodies against Ki-67 and Histone H2AX (phospho-S139) were purchased from Bioworld Technology Co. Ltd. (Nanjing, China).

Lewis lung cancer (LLC) cells were cultured in DMEM (HyClone, Thermo Scientific, Waltham, MA) supplemented with 10% fetal bovine serum (HyClone, Thermo Scientific, Waltham, MA) at 37 °C in a 5% CO_2 incubator.

In vitro Ara-C and irradiation treatments

Different concentrations (0.25 μg/ml to 8 μg/ml) of Ara-C were added to the LLC cells at the logarithmic phase, and the medium was changed after 2 h to remove the drug. After determining the concentration-dependent inhibition of colony formation, the radio-sensitizing ability of a moderately toxic concentration was analyzed. One hour after adding the Ara-C, the cells were irradiated up to 10 Gy using a linear accelerator (Varian) at the dose rate of 60 cGy/min.

Colony forming assay

To assess colony formation, the variously treated Lewis cells were seeded into 6-well plates and cultured for 10–14 days. The cells were then fixed with methanol, stained with 0.5% crystal violet for 20 min, and visible colonies were counted under a microscope (Leica TE2000-S microscope, Tokyo, Japan). Colonies consisting of more than 50 cells were scored as "survivors". Plating efficiency (PE) was calculated as number of colonies divided by number of cells plated, and the surviving fraction (SF) was determined by normalizing PE of the treated cells to that of the control cells. The sensitivity enhancement ratio (SER) was calculated by multi-target model fitting of the data using nonlinear regression.

Preparation of cytarabine hydrogel (Ara-HA-Tyr)

The HA-Tyr solution was prepared by dissolving HA (1000 mg, 2.5 mM) in 100 ml distilled water with continuous stirring at room temperature until the solution was clear. Tyr-HCl (202 mg, 1.2 mM) was added to the above, and the reaction was catalyzed by EDC·HCl (479 mg, 2.5 mM) and NHS (290 mg, 2.5 mM), and the pH was adjusted to 7. The ensuing HA-Tyr solution was dialyzed (molecular weight cut off = 3000), and then lyophilized. The dried HA-Tyr (50 mg) and Ara (250 mg) were dissolved in 5 ml PBS (pH 7.4), followed by the addition of different concentrations of freshly prepared HRP and H_2O_2, and the vials were gently vibrated.

In vitro drug release

To measure Ara-C release from the hydrogel carrier, 1 ml Ara-HA-Tyr (theoretical drug loading rate 5%) with 25 U/ml hyaluronidase and 1 ml 50 mg/ml free Ara-C solution were placed in separate dialysis bags (MWCO: 3.5 kDa), and incubated in 50 ml PBS (pH = 7.4) containing Tween 80 (0.5%, *w/v*) at 37 °C with gentle shaking (100 rpm). At pre-determined time points, 2 ml aliquots were taken from the dialysis bags, and replaced with the same volume of fresh pre-warmed medium. The supernatants were stored at −20 °C, and subsequently analyzed using high-performance liquid chromatography (HPLC, Agilent, USA) with a reverse phase C18

column (4.6 × 50 mm, 3.5 mm particle size). The samples were dissolved in the mobile phase consisting of methanol/PBS (5/95, v/v), and HPLC was performed at the flow rate of 1 ml/min, column temperature 35 °C and detection wave length 250 nm.

Establishment of lung cancer model and treatment protocol

Female C57BL/6J mice (4–6 weeks old) were provided by the Chengdu Dashuo Experimental Animal Center (Chengdu, China). The animals were housed in a specific pathogen free (SPF) room, and provided sterile food pellets and water ad libitum. All animal experiments were implemented in accordance with the Institutional Animal Care and Use Guidelines, and approved by the Institutional Animal Southwest Medical Care and Use Committee (Luzhou, China). A lung cancer model was established by subcutaneously injecting each mouse with a 100 μl suspension of LLC cells (2×10^7 cells/ml) in the dorsal aspect of the right foot. The cells were allowed to grow for 10 days till the tumors volumes were ~100–200 mm^3. The tumor-bearing mice were randomized into the following six treatment groups ($n = 12$ each): control (0.9% normal saline or NS), Ara-C, Ara-HA-Tyr, RT, RT + Ara-C, RT + Ara-HA-Tyr. The Ara-C and Ara-HA-Tyr solutions were injected intra-tumorally at 100 mg/ml or 500 mg/kg in 100 μl once every 2 days for a total of 4 times, based on the doses used in human clinical trials and previous reports [16]. The truncal region of the mice harboring the tumor xenograft were irradiated before the third injection at the dose rate of 60 cGy/min and source–subject distance of 70 cm, to a total dose of 10 Gy. The head and abdominal regions were protected by 0.5 cm thick lead shielding. After treatment, half of the animals in each group were randomly euthanized, and the tumors were harvested for various analyses, along with the eyeballs peripheral blood samples for WBC counts. The remaining mice were observed for tumor growth and survival rate. Changes in body weight were recorded before and after treatment, and the tumor size was measured by calipers (length and width) every two days. The tumor volumes were calculated with the formula $V = a \times b^2 \times \pi/6$, where a is the larger and b is the perpendicular shorter tumor axis. A tumor growth curve was plotted based on tumor size against days after treatment. The mice were observed until death, and the survival time of each mouse was recorded. Tumor growth delay (TGD) was calculated with (Ti_5-T_5) as the time taken for the treated tumors (Ti_5) and the control tumors (T_5) to increase 5-fold relative to their initial volume.

Micro ^{18}F-FDG PET/CT imaging

The metabolic status of the tumors in response to different treatments were evaluated in terms of ^{18}F-FDG uptake, by performing micro PET/CT scans one day after the treatment using Inveon micro PET/CT (Siemens, Munich, Germany). The mice were fasted for 12 h, anesthetized with 1% pentobarbital at the dose of 5 ml/kg, and then injected with 100–200 mCi FDG into their tail veins. One hour after ^{18}F-FDG administration, the mice were placed in a central PET ring field and PET/CT images were acquired using the following parameters: 80 kV, 500 mA, slice thickness 1.5 mm, 10 min per bed position. The image plane with the largest tumor appearance was selected for analysis, and the ROIs were manually drawn across the entire tumor. Tracer uptake values of the tumors were measured in attenuation-corrected lateral chromatographic sections by calculating standard uptake values (SUVs) measured by ROI.

Apoptosis and cell cycle analysis

Soy bean-sized tumors were harvested from the mice, cut into pieces and immediately mixed with 200 μl of 0.25% trypsin/EDTA (1:1, v/v). The tissues were digested at room temperature for 1 min with continuous stirring, and then filtered through a 70-mm nylon mesh filter. The individual tumor cells were harvested by centrifuging at 1500 rpm for 3 min at room temperature, and washed thrice with saline. For the cell cycle analysis, the cells were fixed overnight with 70% ethanol at 4 °C, washed thrice with PBS (0.01 M, pH 7.4), and re-suspended in 50 ng/ml propidium iodide (PI) (Keygen, Nanjing, China) solution containing 20 mg/ml RNaseA. The cells were incubated for 30 min at room temperature, washed, and analyzed by flow cytometry (BD FACSVerse, Piscatway, NJ). For apoptosis analysis, the cells were stained with PI and annexin V-FITC, and the apoptotic cells were detected by flow cytometry (BD FACSVerse, Piscatway, NJ).

Immunohistochemistry (IHC)

The harvested tumors were fixed with 10% neutral buffered formalin, embedded in paraffin, and then cut into 4 μm thick sections. The tissue sections were immuno-stained using antibodies against phosphorylated histone H2AX (γ-H2AX) and Ki-67 according to the manufacturer's instructions (Bioworld Technology, Nanjing, China), and observed under an optical microscope (Leica TE2000-S microscope, Tokyo, Japan). Cells with moderate and strong brown-stained cytoplasm were scored positive, and cells with weak or undetectable staining of the cytoplasm as negative. The Ki-67 positive and total numbers of cells were counted in 5 randomly selected regions in each tumor section under 400x magnification, and the percentage of positive cells was calculated. The expression of γ-H2AX was quantified using the Image-Pro Plus 6.0 software (Media Cybernetics, USA).

Statistical analysis

All data are expressed as the mean ± standard deviation (SD). One-way analysis of variance (ANOVA) was used to compare different groups, and survival curves were plotted according to the Kaplan–Meier method. *P* values less than 0.05 and 0.01 were considered statistically significant. Data analysis was performed using SPSS statistics 17.0 software (SPSS Inc., Chicago, IL).

Results

In vitro toxicity of Ara-C

LLC cells were treated with different concentrations of Ara-C, and the toxicity was evaluated in terms of clonogenic inhibition. As shown in Fig. 1a and c, the surviving clones were reduced to 70% and 10% respectively when treated with 0.5 μg/ml (2.06 nM) and 8 μg/ml (32.9 nM) Ara-C respectively, with a clear survival threshold at 1 μg/ml (4.12 nM). Ara-C doses below 0.5 μg/ml did not significantly affect the survival rate of the LLC cells. Based on these results, the radio-sensitization abilities of the moderately toxic (0.5 μg/ml) and a lower dose (0.25 μg/ml) of Ara-C were tested concomitant to irradiating the cells with 0, 2, 4, 6, 8 and 10Gy X-rays. Ara-C showed significant radio-sensitizing effects at the indicated doses with SERs of 1.148 and 1.619, which resulted in greater clonogenic inhibition compared to cells treated with radiation alone (Fig. 1b and d). In addition, the Dq, D0, and SF2 of the Ara-C and RT combination group (Ara-C + R) were lower than that of the RT group (Table 1). Taken together, Ara-C sensitizes LLC cells to radiotoxicity, resulting in a significant inhibition in colony formation capacity.

Ara-HA-Tyr preparation and in vitro release

HA-Tyr conjugates were successfully crosslinked through the enzyme-mediated coupling of tyramine moieties by H_2O_2 and HRP (Fig. 2). Peroxidase is frequently used as a catalyst for oxidative coupling of phenol derivatives under mild reaction conditions. The Ara-HA-Tyr hydrogel was transparent with a semi-solid nature. Based on the preliminary results, 5% Ara-HA-Tyr was selected for the subsequent in vivo experiments. The in vitro release kinetics of Ara-C from HA-Tyr are shown in Fig. 2c, which clearly indicate that Ara-C was released in a sustained manner. Taken together, HA-Tyr hydrogel-encapsulation can minimize toxicity to healthy tissues and increase drug accumulation in the target area.

RT combination therapy delayed tumor growth

We observed a tumor formation rate of 100% with the LLC cells. To evaluate the anti-tumor efficacy of Ara-HA-Tyr and RT combination, the tumor volumes were measured after treatment (Fig. 3a), and the duration of survival was recorded (Fig. 3b). Tumor growth was respectively delayed for 2 and 5 days in mice treated with Ara-HA-Tyr or RT alone, while the combination of RT + Ara-HA-Tyr resulted in a TGD of 11 days. In addition, the median survival time of the RT + Ara-HA-Tyr group was 60 days, which was significantly longer than the 24.5, 30, 31 and 37 days seen in the control, Ara-HA-Tyr, Ara-C and RT groups respectively. In contrast, mice

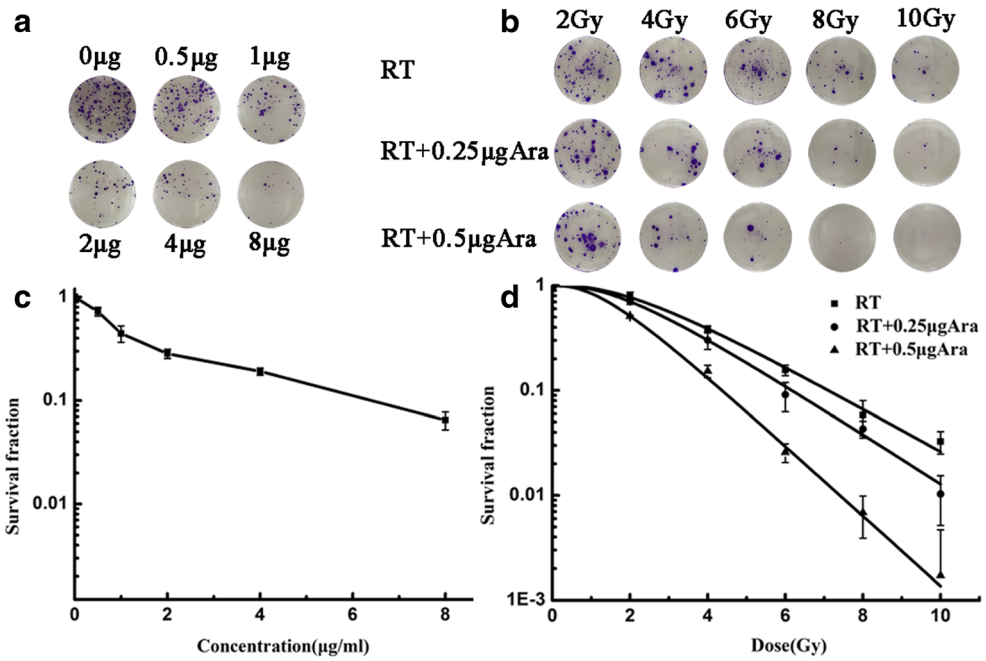

Fig. 1 Clonogenic survival of LLC cells after 2 h exposure to different concentrations of Ara-C (**a**, **c**). Colony formation capacity of LLC cells exposed to different radiation doses alone (square symbols) or in combination with 2 h Ara-C treatment (round and triangular symbols indicate different Ara-C concentrations). Irradiation was always performed 1 h after the addition of Ara-C (**b**, **d**). Data points represent the mean ± standard deviation from at least three independent experiments. The solid curve was obtained by fitting a multi-target model to the data

Table 1 The cell survival rate was measured by colony forming assay in Lewis cell

	D0	Dq	SF2	SER
RT	2.109	2.322	0.771	
RT + 0.25μgAra	1.838	1.998	0.704	1.148
RT + 0.5 μgAra	1.303	1.410	0.511	1.619

in the RT + Ara-C group died in the early stages of treatment, with an average survival duration of only 16 days. Taken together, RT and Ara-HA-Tyr synergistically increased tumor growth inhibition compared to either monotherapy, and encapsulation of the Ara-C reduced its systemic toxicity.

HA-Tyr encapsulation decreased Ara-C toxicity in vivo

Significant differences were seen in the body weights of mice before and after treatment in all groups (Fig. 3c). While the pre-treatment body weights were similar across the groups ($P > 0.05$), the mice in the control, Ara-HA-Tyr and RT groups gained weight by 4.9%, 3.9% and 0.5% respectively post-treatment. The body weight of the RT + Ara-HA-Tyr group mice decreased by ~4.4%, while mice in the Ara-C and RT + Ara-C groups lost 14.3% and 18.3% of their weight respectively. This was consistent with a decrease in water intake and body temperature in those groups.

To assess the safety of the different treatment regimens, the WBC counts of the mice were analyzed (Fig. 3d). Tumor-

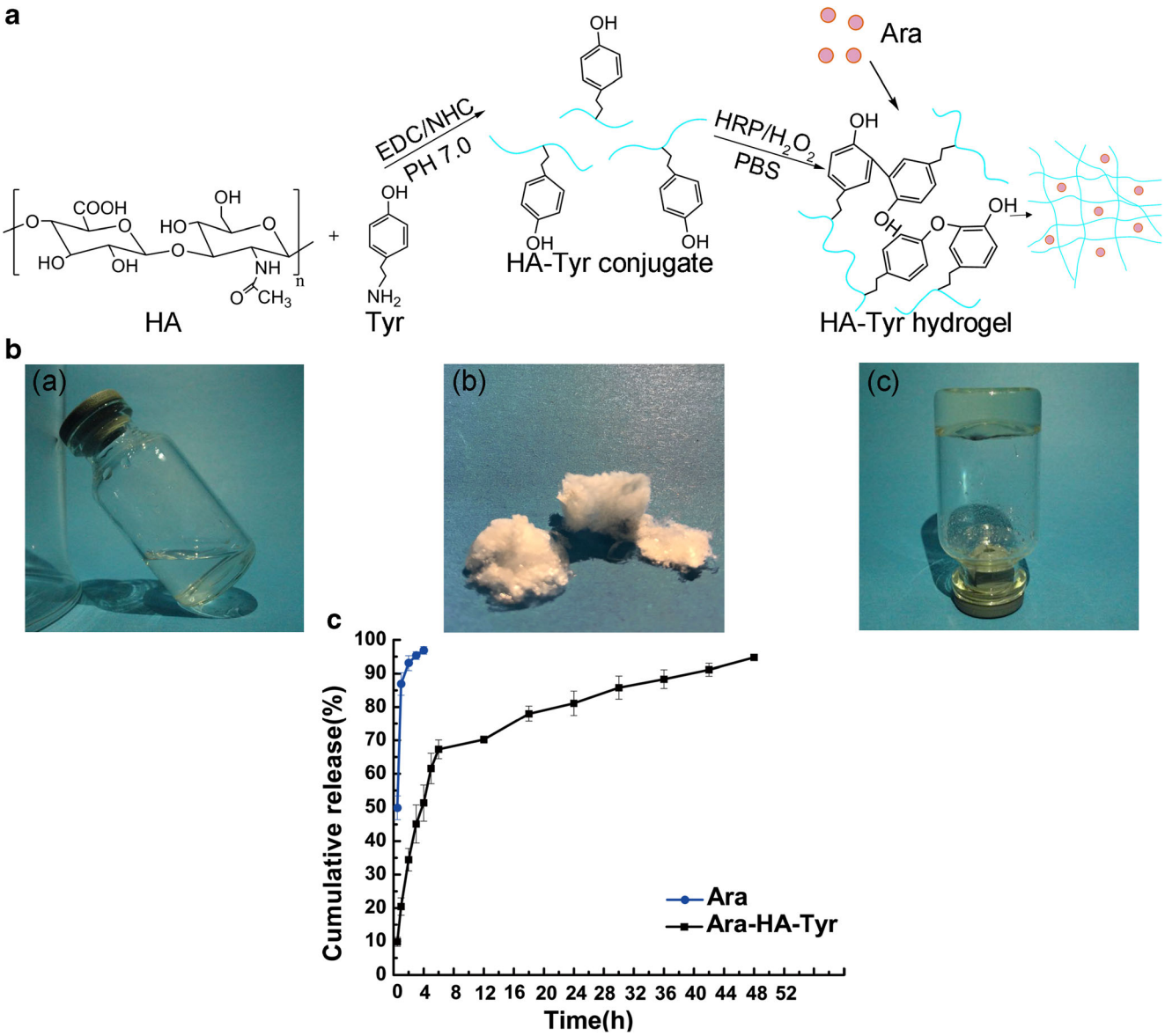

Fig. 2 Ara-HA-Tyr hydrogel preparation. **a** Formation of HA-Tyr conjugates by enzyme-mediated oxidation. **b** Morphology of HA and Tyr (ba), the HA-Tyr conjugate (bb) and the Ara-HA-Tyr hydrogel (bc). **c** In vitro drug release kinetics of free Ara and Ara-HA-Tyr. Data are shown as mean ± SD ($n = 3$)

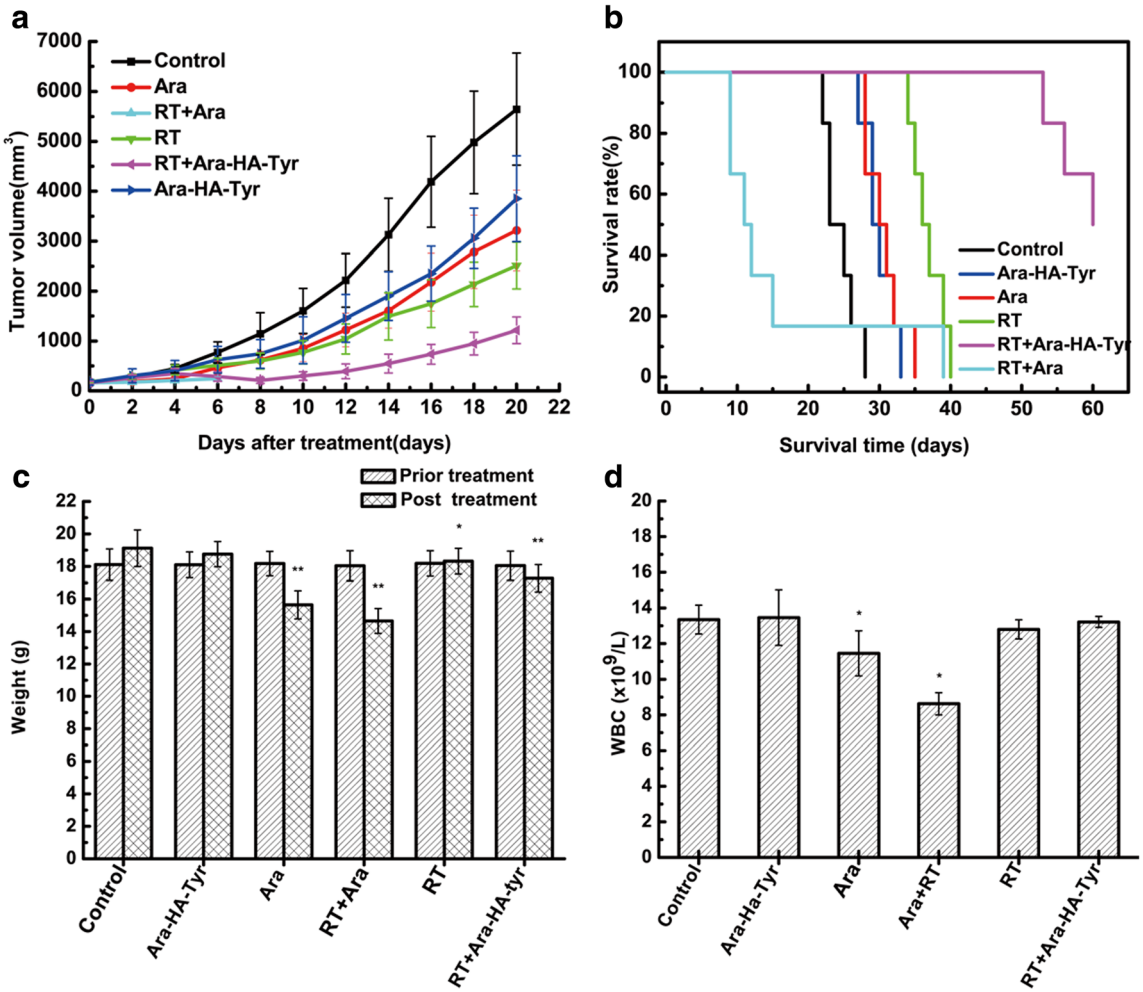

Fig. 3 RT + Ara-HA-Tyr combination inhibited tumor growth in the in vivo LLC model of lung cancer. **a** Suppression of subcutaneous tumor growth by RT + Ara-HA-Tyr. **b** Survival curve of mice in each group. **c** Weight changes in mice before and after treatment. **d** WBC counts in different groups. *$P < 0.05$, ** $p < 0.01$, Ara, RT + Ara, RT and RT + Ara-HA-Tyr compared to control respectively

bearing mice treated with high doses of Ara-C and RT + Ara-C had significantly lower WBCs compared to the control group ($P < 0.05$), while the WBC counts in the Ara-HA-Tyr and RT + Ara-HA-Tyr groups were similar to the control levels. Therefore, the hydrogel encapsulated Ara-C was well tolerated and safe, and not detrimental to the WBCs.

Ara-HA-Tyr and RT combination therapy reduced ^{18}F-FDG uptake

Representative ^{18}F-FDG PET/CT images and the maximal standardized uptake value (SUVmax) of tumor-bearing mice treated with various drug regimens are shown in Fig. 4. Compared to the SUVmax value of the control group (5.73 ± 0.25), that of the Ara-HA-Tyr (3.50 ± 0.26), RT (2.15 ± 0.27) and RT + Ara-HA-Tyr (1.05 ± 0.21) groups were significantly reduced ($P < 0.01$). The lowest SUVmax value in RT + Ara-HA-Tyr group indicates a superior anti-tumor response of the combination therapy compared to either monotherapies.

Ara-HA-Tyr and RT combination therapy caused G2/M-phase arrest and triggered apoptosis in tumor cells

To elucidate the mechanisms associated with Ara-HA-Tyr-mediated enhanced radio-sensitization, the cell cycle distribution and apoptosis rates in tumor cells were assessed. As shown in Fig. 5a, no significant differences were seen in the relative proportion of cells in the G1 phase among the treatment groups ($P > 0.05$). However, the percentage of S-phase cells were significantly decreased in the RT + Ara-HA-Tyr group (36.34 ± 4.38%) compared to the control (47.63 ± 3.07%), Ara-HA-Tyr (49.13 ± 5.27%), Ara-C (51.21 ± 3.06%) and RT (44.38 ± 4.12%) groups (all $P < 0.05$). RT alone and in combination with Ara-HA-Tyr increased the percentage of cells in the G2/M-phase compared to the other

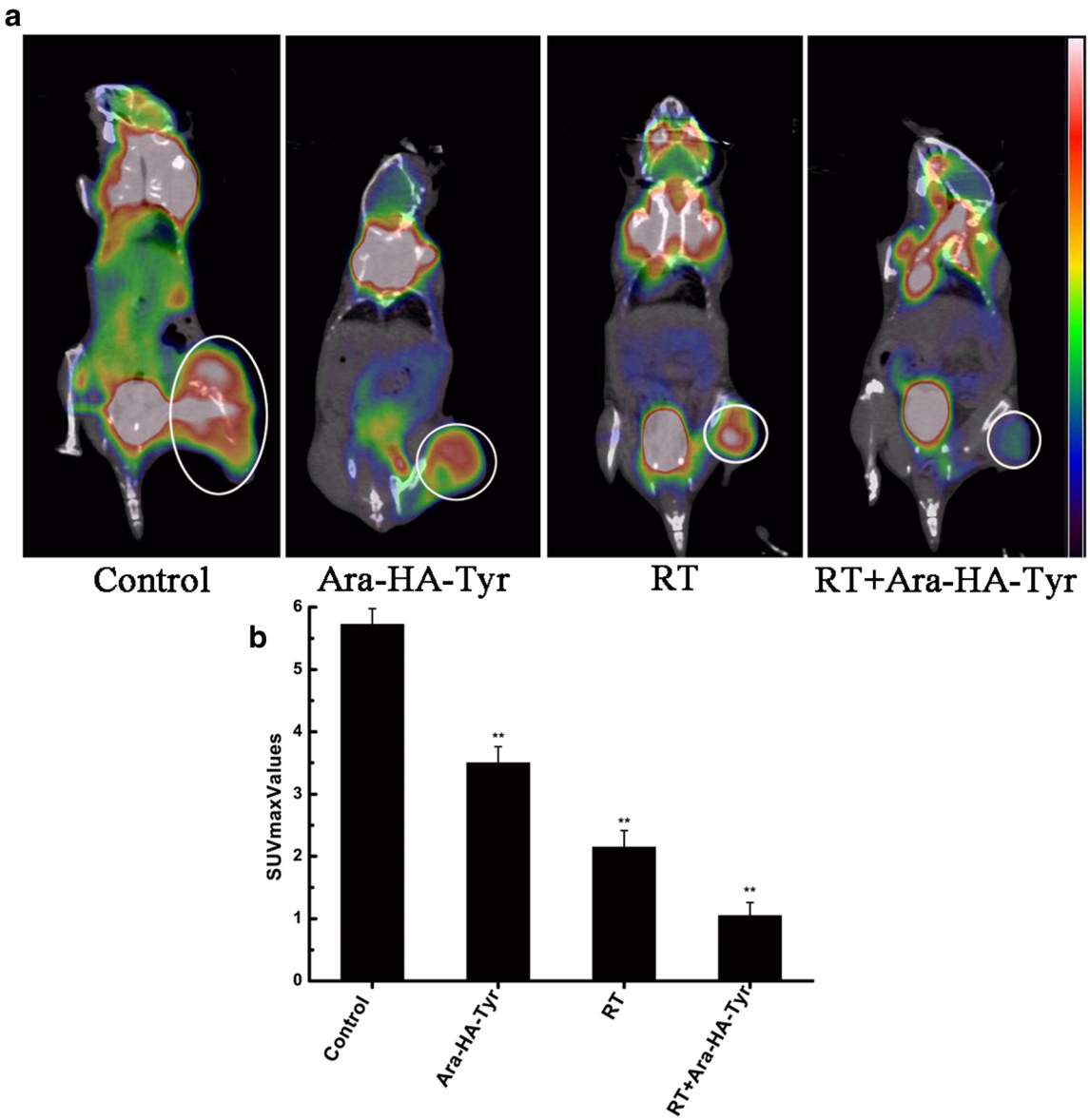

Fig. 4 Representative ^{18}F-FDG PET/CT images of the mice after the last treatment. ** $p < 0.01$, Ara, Ara-HA-Tyr, RT and RT + Ara-HA-Tyr compared to control

groups, with significant differences between these two groups (8.53 ± 3.11% vs 16.28 ± 1.99%; $P < 0.01$) (Fig. 5ca). In addition, RT + Ara-HA-Tyr group had the highest percentage of apoptotic cells (39.36 ± 1.07%), followed by RT (23.78 ± 1.52%), Ara-HA-Tyr (13.10 ± 0.24%), Ara-C (13.99 ± 1.75%) and control (4.44 ± 0.68%) groups (Fig. 5cb), indicating only a slight impact of Ara-C on apoptosis. Figure 5b shows the late apoptotic and dead cells, live cells and early apoptotic cells in the UR, LL and LR corners respectively. The total cell death rate (UR + LR) was significantly higher following RT + Ara-HA-Tyr therapy compared to either monotherapies ($p < 0.01$). Taken together, RT + Ara-HA-Tyr significantly increased the number of cells in the G2/M-phase and decreased that in the S-phase, along with increasing total cell death rate due to apoptosis.

Ara-HA-Tyr and RT combination therapy decreased tumor cell proliferation index and increased DNA damage foci

The effect of the Ara-HA-Tyr and RT combination therapy on tumor cell proliferation and DNA damage was assessed respectively by the expression of Ki-67 (Fig. 6a) and γ-H2AX (Fig. 7a) in tumor tissues. The relative proportion of Ki-67 positive cells was significantly lower in the RT + Ara-HA-Tyr group (27.64 ± 6.95%) compared to the RT (55.87 ± 3.38%), Ara-C (59.89 ± 5.11%), Ara-HA-Tyr (61.99 ± 4.98%) and control (68.31 ± 3.73%) groups (all $p < 0.01$). The control group tumors showed significantly higher proliferation index compared to the RT ($P < 0.05$) and RT + Ara-HA-Tyr ($P < 0.01$) groups (Fig. 6b). In

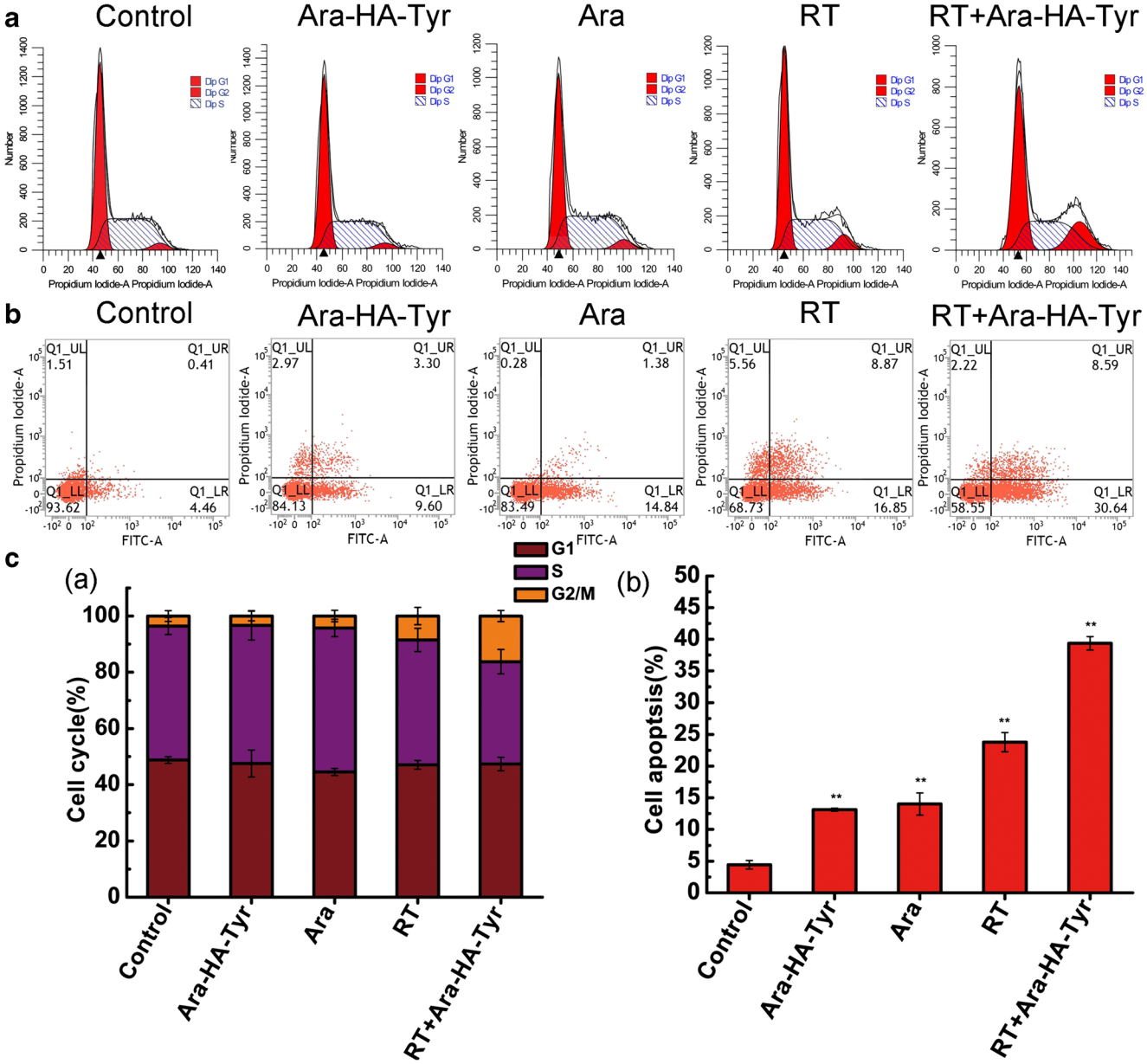

Fig. 5 Analysis of the cell cycle phases (**a**) and apoptosis (**b**). The percentage of cells in the G1, S and G2/M phases (ca) and the percentage of apoptotic cells (cb) in each group were calculated. ** $p < 0.01$, Ara, Ara-HA-Tyr, RT and RT + Ara-HA-Tyr compared to control

addition, a higher number of γ-H2AX positive cells were observed in the tumor tissues of the RT + Ara-HA-Tyr group, followed by the RT, Ara-C, Ara-HA-Tyr and control groups in decreasing order (Fig. 7b; $p < 0.01$), indicating a significant increase in DNA double-strand damage in the RT + Ara-HA-Tyr group.

Discussion

Concurrent radio-chemotherapy (RCT) is a potent therapeutic strategy used for various advanced tumors, including lung cancer [17]. The underlying mechanism is the radiosensitizing effect of the chemotherapeutic drugs which increase tumor cell death and clearance [18]. Cytarabine (Ara-C) is a deoxycytidine analog belonging to a family of antimetabolites. It is phosphorylated by an endogenous kinase and subsequently incorporated into the DNA during polymerase-mediated strand extension, which stalls the replication fork and inhibits DNA synthesis [19, 20]. The toxic effects of nucleoside analogs on tumor cells, such as inhibition of DNA synthesis and repair, apoptosis, cell cycle skewing, interference with nucleotide metabolism and alterations in the intracellular nucleotide pools, are associated with their radiosensitizing abilities [21, 22]. Due to its short half-life and rapid inactivation by DCD outside the target cells, Ara-C is

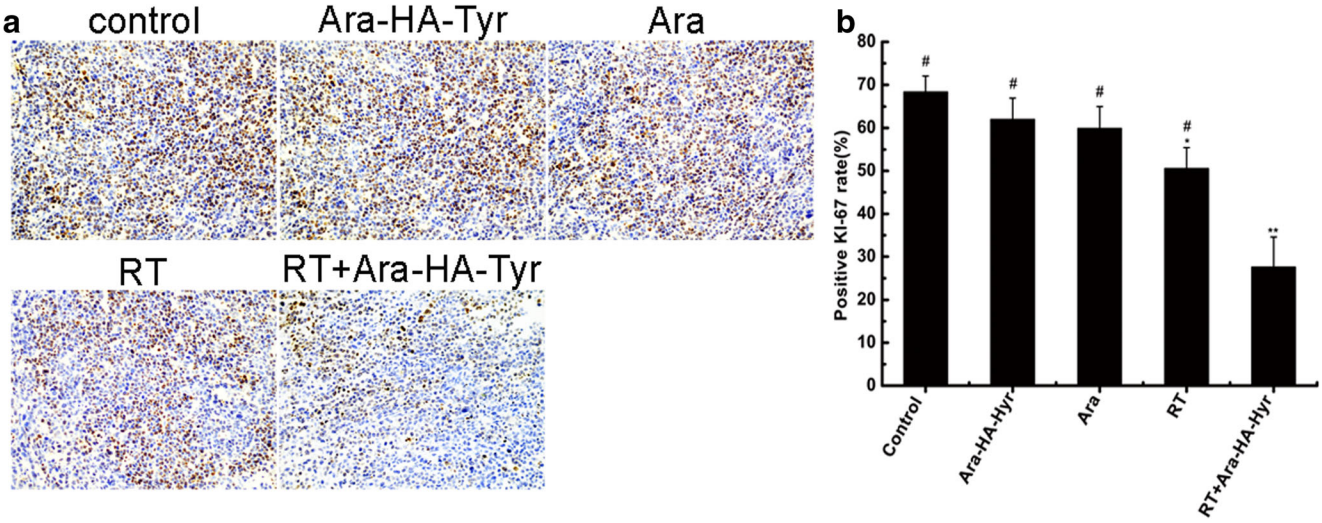

Fig. 6 Ki-67 expression in transplanted tumors from different groups. **a** Representative IHC images showing Ki-67 expression in tumor tissues. Original magnification, ×400. **b** Histogram showing percentage of Ki-67 positive cells in each group. Data are expressed as mean ± SD. $^{\#}P < 0.05$, control, Ara and Ara-HA-Tyr compared to RT + Ara-HA-Tyr; $^{*}P < 0.05$, $^{**}p < 0.01$, RT and RT + Ara-HA-Tyr compared to control

traditionally administered via continuous intravenous infusion or as high-dose infusions over 1–3 h [23].

To elucidate the radio-sensitizing abilities of Ara-C on Lewis lung cancer (LLC) cells, a moderately toxic concentration was combined with different radiation doses. The combination of Ara-C and RT resulted in significantly greater clonogenic inhibition and fewer surviving colonies compared to either therapy alone (Fig. 1). In addition, Ara-C increased radio-sensitivity of the LLC cells in a dose-dependent manner, measured in terms of higher SER and lower Do and Dq (Table 1). The underlying mechanism of Ara-C-induced radio-sensitization can be explained by another study, which showed that the toxicity of gemcitabine against radiation-resistant S-phase cells was mediated by increased apoptosis and DNA repair block [24].

We encapsulated Ara-C in the HA-Tyr hydrogel (Ara-HA-Tyr) to increase its intra-tumoral retention, and maintain an effective in situ drug concentration by slowing its release. The crosslinked polymeric network of the hydrogel acts as a drug depot (Fig. 2a, b), which not only releases Ara-C in a sustained manner, but also protects it from the potentially harsh environment in the vicinity of the release site, such as the presence of deoxycytidine deaminase (DCD), which can rapidly de-aminate Ara-C into an inactive metabolite or Ara-U

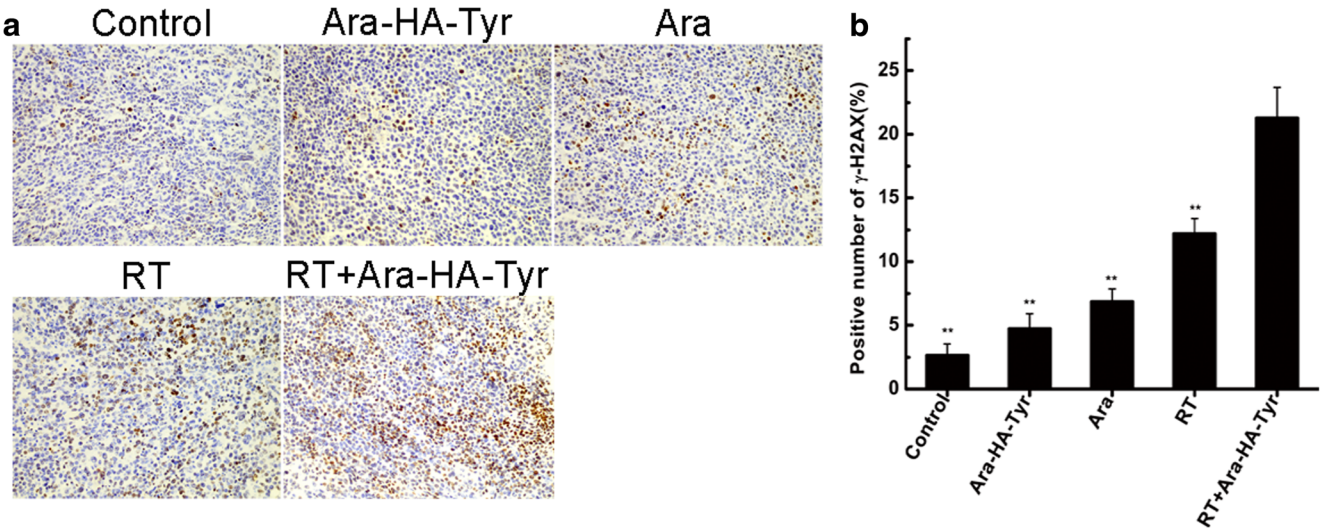

Fig. 7 γ-H2AX expression in transplanted tumors from different groups. **a** Representative IHC images showing γ-H2AX expression in tumor tissues. Original magnification, ×400. **b** Histogram showing percentage of γ-H2AX positive cells in each group. Data are expressed as mean ± SD.$^{**}P < 0.01$, control, Ara, RT and Ara-HA-Tyr compared to RT + Ara-HA-Tyr

[20]. Since free Ara-C was rapidly released from the dialysis bag, we can conclude that the dialysis membrane had no retarding effect on drug release from HA-Tyr. The bound drug showed an initial abrupt release from the surface layer of HA-Tyr, followed by sustained release (Fig. 2c) in the presence of hyaluronidase due to degradation of the hydrogel network [25], and the overall drug release rate after 48 h was 94.77 ± 1.76%. Taken together, the hydrogel-encapsulated Ara-C was released in a highly controlled manner compared to the free Ara-C.

We also tested the radio-sensitization effects of Ara-C in vivo by administering the drug intra-tumorally, since direct injection into the tumor mass can maximize targeted delivery to the tumor cells and minimize systemic toxicity. HA and its derivatives act as sustained-release carriers which delay drug release and prolong drug action in vivo. They have been used to deliver various bio-active substances such as proteins, nucleic acids and anti-neoplastic drugs [26–29]. In addition, HA is well-tolerated and has no serious side effects since it is degraded into water and oxygen by peroxidase/catalase [30]. The basis of the increased targeting and lower side effects of HA-Tyr encapsulated drugs is the high expression of CD44, the receptor for hyaluronic acid, on the surface of tumor cells [31–33]. Although free Ara-C showed slightly higher tumor inhibition compared to Ara-HA-Tyr, due to massive killing of tumor cells by its sudden release, it caused a significant decrease in body weight of the mice (Fig. 3c). Combining RT with free Ara-C resulted in drastic weight loss at the beginning of treatment and a significant decrease in WBCs, along with shorter survival time (Fig. 3c, d). In contrast, the RT + Ara-HA-Tyr group had only slight weight loss and a high survival rate, with the most significant tumor growth delay (Fig. 3a, b). These findings are consistent with previous studies showing improved targeting and lower toxicity of the hyaluronan forms of paclitaxel, doxorubicin etc. [33–36].

Tracking ^{18}F-FDG uptake by PET/CT is widely used for tumor detection, as well as for monitoring therapy. Normal cells and cancer cells differ in glucose metabolism status, a phenomenon known as the Warburg effect, which can be used to distinguish tumors from healthy tissues [37]. A higher FDG uptake in a given tumor indicates higher glucose metabolism, suggesting poor response and poor prognosis, while tumors with lower FDG uptake may have a better response to treatment. Based on this index, RT + Ara-HA-Tyr was most effective in inhibiting tumor metabolism and growth (Fig. 4). Taken together, the sustained release and targeted delivery of Ara-HA-Tyr was responsible for its high anti-tumor efficacy and low systemic toxicity.

The anti-tumor effects of RT + Ara-HA-Tyr can be the result of several cellular and molecular mechanisms, including apoptosis, cell cycle arrest, inhibition of proliferation and DNA damage. Apoptosis is a form of programmed cell death that forms the basis of RT and several chemotherapeutic drugs. The combination of RT and Ara-HA-Tyr synergistically increased apoptosis in the LLC cells, which inhibited tumor growth (Fig. 5b, c). This is consistent with studies showing that gemcitabine depletes dATP pools in the S phase, leading to misincorporation and misrepair of bases which, if not correctly repaired before irradiation, augments the cytotoxic effects of ionizing radiation [19, 38]. In addition, nucleoside analogs including Ara-C primarily target the S-phase and block cell division [39]. Consistent with this, tumors treated with Ara-C or Ara-HA-Tyr had a higher percentage of cells in the S-phase compared to the control group, indicating arrest or delay of cell cycle progression during S phase. The combination of Ara-HA-Tyr and RT decreased the number of cells in the S-phase (36.34 ± 4.38%) by RT-induced apoptosis, and increased that in the G2/M-phase (16.28 ± 1.99%), the most radiosensitive phase of the cell cycle [2], via cell cycle arrest compared to the control group (S: 47.63 ± 3.07%, G2/M: 3.57 ± 1.90%, $P < 0.01$) (Fig. 5a, c). Furthermore, Ara-C can inhibit the repair of radiation-induced sublethal DNA damage. In higher eukaryotes, the preferred donor sequence for recombination is a sister chromatid that limits the homologous recombination repair (HRR) in the S and G2 phases of the cell cycle [40]. The arabinoside–nucleoside analogs inhibit HHR mostly in the S and G2 phases [41], which is consistent with the selective targeting of this pathway by gemcitabine [38, 39]. This could be an additional mechanism of the increased radio-sensitivity of LLCs during RCT.

The synergistic effect of Ara-HA-Tyr and RT on tumor cell proliferation and DNA damage was also analyzed by respectively detecting the expression levels of Ki67 and γ-H2AX. Ki67 is a nuclear antigen associated with proliferation, and RT + Ara-HA-Tyr caused a significant reduction in the percentage of Ki67 positive cells in the tumor xenografts (Fig. 6). This could be the result of Ara-C-mediated inhibition of DNA synthesis at the S phase, along with RT-mediated mitotic inhibition. DNA damage leads to phosphorylation of H2AX on the γ-site of serine139 resulting in γ-H2AX foci in the nuclei [42]. Furthermore, DNA is the primary target of ionizing radiation, which causes base damage, sugar damage, SSBs (single-strand breaks) and DSBs (double-strand breaks), with the latter even triggering cell death [43]. Tumor cells treated with Ara-HA-Tyr and RT showed increased γ-H2AX foci, indicating enhanced DSBs in the LLC cells (Fig. 7). Based on our findings, we hypothesize that Ara-C inhibits radiation-induced SSB and DSB repair by inhibiting DNA polymerase and ribonucleotide reductase, and interfering with nucleotide incorporation during DNA synthesis.

Conclusions

Ara-C was successfully incorporated into the injectable HA-Tyr hydrogel, and the combination of Ara-HA-Tyr and

radiotherapy significantly inhibited lung tumor growth and prolonged the survival of tumor-bearing mice. Ara-HA-Tyr is a potent radiosensitizing agent that enhances apoptosis, G2/M phase arrest and DNA damage in tumor cells.

Funding This work was supported by grants from the National Natural Science Foundation of China (No.81201682), the Scientific Research Foundation of the Luzhou Science and Technology Bureau (No.2016LZXNYD-J05), and the Southwest Medical University Foundation (No.201617).

Compliance with ethical standards

Conflict of interest The authors declare that they have no conflict of interest.

Ethical approval No studies were conducted on human participants. All applicable international, national, and/or institutional guidelines for the care and use of animals were followed. All animal experiments were implemented in accordance with the Institutional Animal Care and Use Guidelines, and approved by the Institutional Animal Southwest Medical Care and Use Committee (Luzhou, China).

Informed consent For this type of study, formal consent is not required.

Publisher's note Springer Nature remains neutral with regard to jurisdictional claims in published maps and institutional affiliations.

References

1. Bernier J, Hall EJ, Giaccia A (2004) Radiation oncology: a century of achievements. Nat Rev Cancer 49:737–747. https://doi.org/10.1038/nrc1451
2. Linam J, Yang LX (2015) Recent developments in radiosensitization. Anticancer Res 355:2479–2485
3. Schiffer CA (2014) Optimal dose and schedule of consolidation in AML: is there a standard? Best Pract Res Clin Haematol 273-4: 259–264. https://doi.org/10.1016/j.beha.2014.10.007
4. Rusch VW, Figlin R, Godwin D, Piantadosi S (1991) Intrapleural cisplatin and cytarabine in the management of malignant pleural effusions: a lung Cancer study group trial. J Clin Oncol 92:313–319. https://doi.org/10.1200/jco.1991.9.2.313
5. Karami L, Jalili S (2015) Effects of cholesterol concentration on the interaction of cytarabine with lipid membranes: a molecular dynamics simulation study. J Biomol Struct Dyn 336:1254–1268. https://doi.org/10.1080/07391102.2014.941936
6. Benesch M, Urban C (2008) Liposomal cytarabine for leukemic and lymphomatous meningitis: recent developments. Expert Opin Pharmacother 92:301–309. https://doi.org/10.1517/14656566.9.2.301
7. Spriggs DR, Robbins G, Takvorian T et al (1985) Continuous infusion of high-dose 1-beta-D-arabinofuranosylcytosine: a phase I and pharmacological study. Cancer Res 458:3932–3936
8. Liao YH, Jones SA, Forbes B, Martin GP, Brown MB (2005) Hyaluronan: pharmaceutical characterization and drug delivery. J Drug Deliv 126:327–342. https://doi.org/10.1080/10717540590952555
9. Wang J, Wang X, Cao Y, Huang T, Song D-X, Tao H-R (2018) Therapeutic potential of hyaluronic acid/chitosan nanoparticles for the delivery of curcuminoid in knee osteoarthritis and an in vitro evaluation in chondrocytes. Int J Mol Med. https://doi.org/10.3892/ijmm.2018.3817
10. Lokeshwar VB, Mirza S, Jordan A (2014) Targeting hyaluronic acid family for cancer chemoprevention and therapy. Adv Cancer Res 123:35–65. https://doi.org/10.1016/b978-0-12-800092-2.00002-2
11. Lin WJ, Lee WC (2018) Polysaccharide-modified nanoparticles with intelligent CD44 receptor targeting ability for gene delivery. Int J Nanomedicine 13:3989–4002. https://doi.org/10.2147/ijn.s163149
12. Hatefi A, Amsden B (2002) Biodegradable injectable in situ forming drug delivery systems. J Control Release 801-3:9–28
13. Kretlow JD, Klouda L, Mikos AG (2007) Injectable matrices and scaffolds for drug delivery in tissue engineering. Adv Drug Deliv Rev 594-5:263–273. https://doi.org/10.1016/j.addr.2007.03.013
14. Kurisawa M, Chung JE, Yang YY, Gao SJ, Uyama H (2005) Injectable biodegradable hydrogels composed of hyaluronic acid-tyramine conjugates for drug delivery and tissue engineering. Chem Commun 34:4312–4314. https://doi.org/10.1039/b506989k
15. Lee F, Chung JE, Kurisawa M (2008) An injectable enzymatically crosslinked hyaluronic acid–tyramine hydrogel system with independent tuning of mechanical strength and gelation rate. J Soft Matter 44:880. https://doi.org/10.1039/b719557e
16. Koga K, Iizuka E, Sato A, Ekimoto H, Okada M (1995) Characteristic antitumor activity of cytarabine ocfosfate against human colorectal adenocarcinoma xenografts in nude mice. Cancer Chemother Pharmacol 366:459–462. https://doi.org/10.1007/bf00685794
17. Skrzypski M, Jassem J (2018) Consolidation systemic treatment after radiochemotherapy for unresectable stage III non-small cell lung cancer. Cancer Treat Rev 66:114–121. https://doi.org/10.1016/j.ctrv.2018.04.001
18. Lawrence TS, Blackstock AW, McGinn C (2003) The mechanism of action of radiosensitization of conventional chemotherapeutic agents. Semin Radiat Oncol 131:13–21. https://doi.org/10.1053/srao.2003.50002
19. Hirata N, Fujisawa Y, Tanabe K, Harada H, Hiraoka M, Nishimoto SI (2009) Radiolytic activation of a cytarabine prodrug possessing a 2-oxoalkyl group: one-electron reduction and cytotoxicity characteristics. Org Biomol Chem 74:651–654. https://doi.org/10.1039/b816194a
20. Reese ND, Schiller GJ (2013) High-dose cytarabine (HD araC) in the treatment of leukemias: a review. Curr Hematol Malig Rep 82: 141–148. https://doi.org/10.1007/s11899-013-0156-3
21. Ewald B, Sampath D, Plunkett W (2008) Nucleoside analogs: molecular mechanisms signaling cell death. Oncogene 2750:6522–6537. https://doi.org/10.1038/onc.2008.316
22. McGinn CJ, Lawrence TS (2001) Recent advances in the use of radiosensitizing nucleosides. Semin Radiat Oncol 114:270–280
23. Tsesmetzis N, Paulin CBJ, Rudd SG, Herold N (2018) Nucleobase and nucleoside analogues: resistance and re-sensitisation at the level of pharmacokinetics, Pharmacodynamics and Metabolism. Cancers (Basel) 107:240. https://doi.org/10.3390/cancers10070240
24. Lawrence TS, Chang EY, Hahn TM et al (1997) Delayed radiosensitization of human colon carcinoma cells after a brief exposure to 2',2'-difluoro-2'-deoxycytidine (Gemcitabine). Clin Cancer Res 35:777–782
25. Lee F, Chung JE, Kurisawa M (2009) An injectable hyaluronic acid-tyramine hydrogel system for protein delivery. J Control Release 1343:186–193. https://doi.org/10.1016/j.jconrel.2008.11.028
26. Huang G, Huang H (2018) Hyaluronic acid-based biopharmaceutical delivery and tumor-targeted drug delivery system. J Control Release 278:122–126. https://doi.org/10.1016/j.jconrel.2018.04.015

27. Wu JL, Tian GX, Yu WJ, Jia GT, Sun TY, Gao ZQ (2016) pH-responsive hyaluronic acid-based mixed micelles for the hepatoma-targeting delivery of doxorubicin. Int J Mol Sci 174:364. https://doi.org/10.3390/ijms17040364
28. Kim A, Checkla DM, Dehazya P et al (2003) Characterization of DNA-hyaluronan matrix for sustained gene transfer. J Control Release 901:81–95
29. Qin Y, Tian Y, Liu Y, Li D, Zhang H, Yang Y, Qi J, Wang H, Gan L (2018) Hyaluronic acid-modified cationic niosomes for ocular gene delivery: improving transfection efficiency in retinal pigment epithelium. J Pharm Pharmacol 709:1139–1151. https://doi.org/10.1111/jphp.12940
30. Ogawa Y, Kubota K, Ue H et al (2009) Phase I study of a new radiosensitizer containing hydrogen peroxide and sodium hyaluronate for topical tumor injection: a new enzyme-targeting radiosensitization treatment, Kochi Oxydol-radiation therapy for Unresectable carcinomas, type II (KORTUC II). Int J Oncol 343: 609–618
31. Jordan AR, Racine RR, Hennig MJ et al (2015) The role of CD44 in disease pathophysiology and targeted treatment. Front Immunol 6: 182. https://doi.org/10.3389/fimmu.2015.00182
32. Yang Y, Zhao Y, Lan J, Kang Y, Zhang T, Ding Y, Zhang X, Lu L (2018) Reduction-sensitive CD44 receptor-targeted hyaluronic acid derivative micelles for doxorubicin delivery. Int J Nanomedicine 13:4361–4378. https://doi.org/10.2147/ijn.s165359
33. Yoon HY, Koo H, Choi KY, Lee SJ, Kim K, Kwon IC, Leary JF, Park K, Yuk SH, Park JH, Choi K (2012) Tumor-targeting hyaluronic acid nanoparticles for photodynamic imaging and therapy. Biomaterials 3315:3980–3989. https://doi.org/10.1016/j.biomaterials.2012.02.016
34. Xiong H, Ni J, Jiang Z, Tian F, Zhou J, Yao J (2018) Intracellular self-disassemble polysaccharide nanoassembly for multi-factors tumor drug resistance modulation of doxorubicin. Biomater Sci 69: 2527–2540. https://doi.org/10.1039/c8bm00570b
35. Saravanakumar G, Choi KY, Yoon HY, Kim K, Park JH, Kwon IC, Park K (2010) Hydrotropic hyaluronic acid conjugates: synthesis, characterization, and implications as a carrier of paclitaxel. Int J Pharm 3941-2:154–161. https://doi.org/10.1016/j.ijpharm.2010.04.041
36. Zhao T, He Y, Chen H, Bai Y, Hu W, Zhang L (2017) Novel apigenin-loaded sodium hyaluronate nano-assemblies for targeting tumor cells. Carbohydr Polym 177:415–423. https://doi.org/10.1016/j.carbpol.2017.09.007
37. Fang JS, Gillies RD, Gatenby RA (2008) Adaptation to hypoxia and acidosis in carcinogenesis and tumor progression. Semin Cancer Biol 185:330–337. https://doi.org/10.1016/j.semcancer.2008.03.011
38. Shewach DS, Lawrence TS (2007) Antimetabolite radiosensitizers. J Clin Oncol 2526:4043–4050. https://doi.org/10.1200/jco.2007.11.5287
39. Sarkisjan D, van den Berg J, Smit E, Lee YB, Kim DJ, Peters GJ (2016) The radiosensitizing effect of fluorocyclopentenyl-cytosine (RX-3117) in ovarian and lung cancer cell lines. Nucleosides Nucleotides Nucleic Acids 3510-12:619–630. https://doi.org/10.1080/15257770.2016.1216565
40. Heyer WD, Ehmsen KT, Liu J (2010) Regulation of homologous recombination in eukaryotes. Annu Rev Genet 44:113–139. https://doi.org/10.1146/annurev-genet-051710-150955
41. Magin S, Papaioannou M, Saha J, Staudt C, Iliakis G (2015) Inhibition of homologous recombination and promotion of mutagenic repair of DNA double-Strand breaks underpins Arabinoside-nucleoside analogue Radiosensitization. Mol Cancer Ther 146: 1424–1433. https://doi.org/10.1158/1535-7163.mct-14-0682
42. Thiemann M, Oertel S, Ehemann V et al (2012) In vivo efficacy of the histone deacetylase inhibitor suberoylanilide hydroxamic acid in combination with radiotherapy in a malignant rhabdoid tumor mouse model. Radiat Oncol 7:52. https://doi.org/10.1186/1748-717x-7-52
43. Nickoloff JA (2017) Paths from DNA damage and signaling to genome rearrangements via homologous recombination. Mutat Res 806:64–74. https://doi.org/10.1016/j.mrfmmm.2017.07.008